Acta Physica Polonica B Proceedings Supplement **18**, 5-A20 (2025)

TOP-QUARK PHYSICS HIGHLIGHTS FROM ATLAS*

D.E. Martins

on behalf of the ATLAS Collaboration

Institute of Nuclear Physics Polish Academy of Sciences
Radzikowskiego 152, 31-342 Kraków, Poland

Received 16 April 2025, accepted 16 April 2025,
published online 26 June 2025

The extensive top-quark samples collected by the ATLAS experiment at the LHC have enabled precise measurements of the top-quark production cross section, reaching unprecedented accuracy and extending into previously unexplored kinematic regimes. These datasets have also provided new insights into top-quark properties, facilitated the observation of rare production processes predicted by the Standard Model, and led to significant advancements in searches within the top-quark sector. This contribution presents key highlights from the ATLAS top-quark physics program, showcasing the latest measurements and emphasizing the sector's broad scientific potential.

DOI:10.5506/APhysPolBSupp.18.5-A20

1. Introduction

Recent findings from the top-quark sector offer an excellent framework for examining the Standard Model (SM) of particle physics. At particle colliders, the production and decay of the top quark involve a complex interplay between electroweak interactions, quantum chromodynamics (QCD) [1], and the Higgs boson [2]. The top quark holds a unique position within the SM due to its weak mixing with quarks other than the bottom quark and its mass, which is roughly 2.1 times that of a W boson and about 1.4 times that of the Higgs boson, making it the heaviest known elementary particle [3]. As it is heavier than the W boson, it is the only quark that decays into a real W boson and a b-quark. This results in a lifetime shorter than the timescale of strong interactions, preventing it from hadronizing or forming bound states. In this respect, the top is the only quark that, in its brief life, behaves as a free one. Due to its large mass and the Yukawa coupling

* Presented at the 31[st] Cracow Epiphany Conference on the *Recent LHC Results*, Kraków, Poland, 13–17 January, 2025.

to the Higgs boson, it also gives important contributions (via loops) to SM precision observables measured at lower scales. The distinct features of the top quark set it apart from other members of its particle family and give it a unique role in the radiative corrections affecting the Higgs mass. Moreover, many SM extensions suggest novel interactions within the top-quark sector, highlighting the significance of conducting measurements in this field.

This contribution outlines important findings from the latest ATLAS [4] studies concerning top-quark production, its characteristics, and interactions with the Higgs boson, along with investigations for New Physics within the top sector. These findings utilize data from proton–proton collisions at a centre-of-mass energy of 13 TeV, gathered throughout the entire Run 2 of the LHC (2015–2018) [5], corresponding to a total integrated luminosity of 140 fb^{-1}. Additionally, dedicated runs were conducted to investigate top-quark pair production in heavy-ion collisions, including lead–lead interactions with an integrated luminosity of 1.9 nb^{-1} at a centre-of-mass energy of $\sqrt{s_{NN}} = 5.02$ TeV (2015 and 2018) and proton–lead with 165 nb^{-1} at $\sqrt{s_{NN}} = 8.16$ TeV (2016).

The results are categorized into three main sections: *(i)* measurements of inclusive and differential top-quark pair production rates; *(ii)* investigations of novel physics related to the spin properties of the top quark; and *(iii)* studies of top-quark pair production in lead–lead and proton–lead collisions.

2. Inclusive measurements

In Ref. [6], the ATLAS Collaboration presents a precise measurement of the single top quark associated with a W boson for a centre-of-mass energy of 13 TeV. The analysis considers only events with two oppositely charged leptons (an electron and a muon). The leading jet is required to satisfy $p_{\mathrm{T}} > 27$ GeV, and events are rejected if a third lepton is present with $p_{\mathrm{T}} > 20$ GeV. Additionally, at least one jet identified as a b-jet, *i.e.*, originating from a b-quark, is required, with $p_{\mathrm{T}} > 20$ GeV and $|\eta| < 2.5$. This event topology is essential for isolating the tW signal from spurious processes, particularly the dominant $t\bar{t}$ background. The selected objects are categorized based on jet and b-jet multiplicities.

The results are reported in three distinct final-state topologies: *(i)* events with exactly one selected jet that is also b-tagged ($1j1b$), *(ii)* events with exactly two selected jets, one of which is b-tagged ($2j1b$), and *(iii)* events with exactly two jets, both b-tagged ($2j2b$). The third category plays a crucial role in constraining the normalization of the $t\bar{t}$ background. To extract the signal, a multivariate analysis approach incorporating boosted decision trees (BDTs) was employed in each of the considered regions to distinguish the tW signal from the background.

This method enhances the measurement sensitivity and enables a more precise determination of the tW cross section. The leading systematic uncertainties arise from $t\bar{t}$ modelling, the jet energy scale, and the reconstruction and calibration of missing transverse energy, $E_{\mathrm{T}}^{\mathrm{miss}}$ (MET), with fractional impacts of 13.2%, 12.0%, and 11.0%, respectively, on the total uncertainty. Additionally, the jet energy resolution and jet flavour tagging contribute with smaller relative impacts of 7.9% and 7.0%. The reported cross section for the tW production is $\sigma_{tW} = 75^{+15}_{-14}$ pb $= 75 \pm 1(\mathrm{stat.})^{+15}_{-14}(\mathrm{syst.}) \pm 1(\mathrm{lumi.})$ pb, which is in good agreement with the SM expectation: $\sigma_{tW}^{\mathrm{theory}} = 79.3^{+1.9}_{-1.8}(\mathrm{scale}) \pm 2.2(\mathrm{PDF})$ pb. The analysis also includes a determination of the left-handed form factor at the W_{tb} vertex $|f_{\mathrm{LV}}V_{tb}| = 0.97 \pm 0.10$.

The analysis of $t\bar{t}$ production accompanied by extra b-jets in the $e\mu$ final state from proton–proton collisions at a centre-of-mass energy of 13 TeV is reported in Ref. [7]. In this study, the fiducial cross section is measured for a final state that includes one electron and one muon, featuring at least three or four b-jets. Leptons are required to have the transverse momentum, $p_{\mathrm{T}} >$ 25 GeV and pseudorapidity $|\eta| < 2.5$, with specific exclusion for electrons in the transition regions $1.37 < |\eta| < 1.52$.

The differential cross sections are measured for different scenarios: events with at least three b-jets ($\geq 3b$) and four b-jets ($\geq 4b$), as well as events featuring three or four b-jets along with at least one additional light jet ($\geq 3b \geq 1l/c$) and ($\geq 4b \geq 1l/c$), respectively. It is worth pointing out that a dedicated measurement of $t\bar{t}$ associated with c-jets, $t\bar{t} + 1c$, and $t\bar{t}+ \geq 2c$, was performed separately, and the results are given in Ref. [8]. Several background sources are considered, including prompt leptons from the $t\bar{t}X$ production ($X = Z, W, H$) and rare SM processes such as tWZ, tWH, $tHbj$, tZ, and $t\bar{t}t\bar{t}$. In addition, backgrounds arising from mis-tagged jets are taken into account, particularly from $t\bar{t}c$ (events containing charm jets) and $t\bar{t}l$ (events with light-flavour jets, *i.e.*, those not containing a c-hadron and a b-hadron).

Figure 1 shows the fiducial cross sections for all configurations together with predictions of several Monte Carlo (MC) generators. The precision for these cross sections is 8.5%, 10%, 13%, and 16%, respectively. The dominant systematics are related to b-tagging, jet energy scale, and $t\bar{t}$ modelling.

The measured fiducial cross sections are compared with various theoretical predictions, and are found to have good compatibility with $t\bar{t}bb$ matrix element predictions, particularly in the regions with at least four b-jets.

The measurement of differential cross sections for $t\bar{t}$ and $t\bar{t}$ + jets processes is conducted within the e/μ+jets channel [9]. Leptons are required to have $p_{\mathrm{T}} > 27$ GeV. The main background processes include single-top production (in t- and s-channels), W+jets, and Z+jets. Additionally, diboson

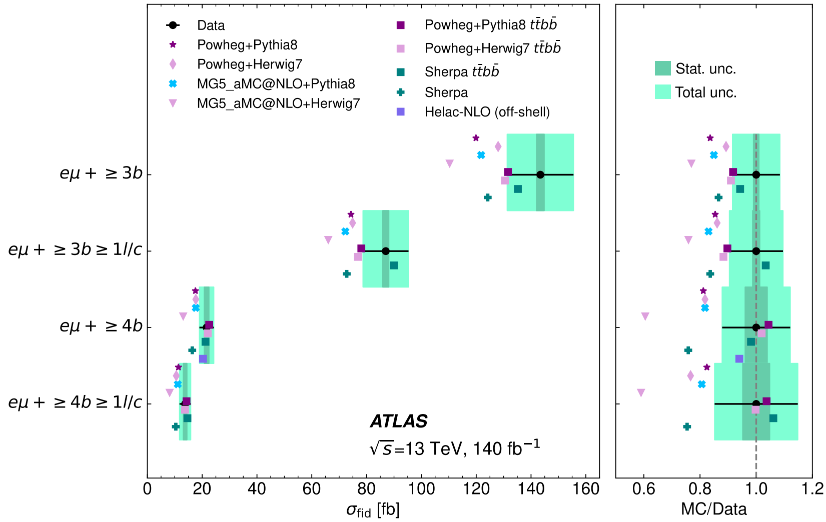

Fig. 1. Measured fiducial cross section for $e\mu + \geq 3b$, $e\mu + \geq 3b \geq 1l/c$, $e\mu + \geq 4b$, and $e\mu + \geq 4b \geq 1l/c$ compared with the central values predicted by different MC generators. The inner (dark) uncertainty band represents the statistical uncertainty in the data, and the outer (light) band includes all uncertainties from both instrumental and theoretical sources [7].

events from WW, ZZ, and WZ decays (both hadronic and leptonic) were taken into account. Differential cross sections are provided at the particle level as functions of various jet observables, such as angular correlations, jet transverse momentum, and invariant masses of final-state jets, highlighting the kinematics and dynamics of the $t\bar{t}$ pair and hard QCD radiation with jets. Figure 2 shows the differential cross section as a function of the jet transverse momenta for $t\bar{t}$ and $t\bar{t} + 1$ jet decay modes.

The primary source of uncertainty in the $t\bar{t}$ channel arises from the b-tagging calibration, which is around 7%. In contrast, the uncertainties for the $t\bar{t} + 1$ jet and $t\bar{t} + 2$ jets processes are mainly influenced by the energy scale and the detector resolution, and are estimated to be approximately 10% and 13%, respectively. These findings significantly enhance the NNLO QCD predictions. Additionally, this marks the first time when a direct comparison of the NNLO-calculated and the experimentally measured cross sections is possible[1].

[1] Recently, predictions for the $t\bar{t}$ production at NNLO QCD have become available and the interface with the parton shower provided by PYTHIA via the MiNNLOPS matching scheme allows for the computation of differential cross sections for jet observables such as those presented in this paper.

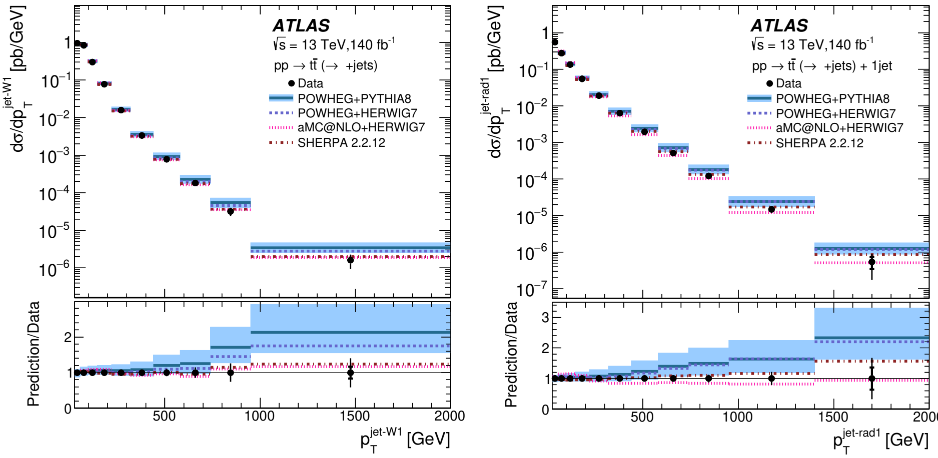

Fig. 2. Differential cross sections as a function of the transverse momentum of the jets for a centre-of-mass energy of 13 TeV considering two decay modes: $t\bar{t}$ (left panel) and $t\bar{t}+1$ jet [9]. The variable $p_{\mathrm{T}}^{\text{jet-W1}}$ denotes one of the two jets used in the hadronic reconstruction of the top quark, while $p_{\mathrm{T}}^{\text{jet-rad1}}$ refers to the highest-p_{T} jet not associated with the reconstructed $t\bar{t}$ system.

The $t\bar{t}$ production in association with a photon and a search for New Physics in the context of SM Effective Field Theory (SMEFT) is conducted in Ref. [10]. The inclusive fiducial cross section for the $t\bar{t}\gamma$ production process is measured, along with differential cross sections in both single-lepton and dilepton decay channels. The predictions of the NLO simulations (MadGraph5_aMC@NLO + PYTHIA 8 and Herwig 7) are compared to the experimental results.

The single-lepton channel selection requires exactly one lepton (e or μ), at least four jets (with at least one identified as a b-jet), and exactly one photon with $E_{\mathrm{T}} > 20$ GeV and $|\eta| < 2.37$ (excluding $1.37 < |\eta| < 1.52$). The double-lepton channel selection requires exactly two leptons (e or μ), at least four jets (with at least two identified as b-jets), exactly one photon with $E_{\mathrm{T}} > 20$ GeV and $|\eta| < 2.37$ (excluding $1.37 < |\eta| < 1.52$), and MET greater than 30 GeV. The largest prompt photon background contribution arises from $t\bar{t}\gamma$ decay events, contributing about 30% (45%) of the total number of events in the single-lepton (dilepton) channel. All other background processes with a prompt photon ($tW\gamma$, single-top quark, $V\gamma$, VV, $t\bar{t}V$, and $t\bar{t}$) constitute about 15% of the selected events in both channels.

The measured cross section for the $t\bar{t}\gamma$ production, obtained as a free parameter in the profile-likelihood fit, for the single lepton channel is given by $\sigma_{t\bar{t}\gamma}^{\text{single lep.}} = 288^{+21}_{-19} = 288 \pm 5(\text{stat.})^{+20}_{-19}(\text{syst.})$ fb, showing a good agreement with the expected SM cross section $255^{+25}_{-26}(\text{scale})^{+6}_{-4}(\text{PDF})$ fb. For all decay modes, the cross section is $\sigma_{t\bar{t}\gamma}^{\text{single lep.}} = 704^{+49}_{-46} = 704 \pm 5(\text{stat.})^{+49}_{-46}(\text{syst.})$ fb. The primary sources of uncertainty pertain to the modelling of $t\bar{t}\gamma$ production at 5.1%, as well as the experimental uncertainties in jet and b-tagging, which are 3.5% and 2.6%, correspondingly. In the dilepton channel, the cross section is measured as $\sigma_{t\bar{t}\gamma}^{\text{dilep.}} = 45.7^{+3.3}_{-3.1} = 45.7^{+1.4}_{-1.3}(\text{stat.})^{+3.0}_{-2.8}(\text{syst.})$ fb, aligning with the MC prediction of $40.9^{+3.9}_{-4.0}(\text{scale})^{+0.9}_{-0.5}(\text{PDF})$ fb. Taking into account all decay modes, the resulting cross section is $\sigma_{t\bar{t}\gamma}^{\text{dilep.}} = 116.1^{+8.2}_{-7.7} = 116.1 \pm 1.7(\text{stat.})^{+8.0}_{-7.6}(\text{syst.})$ fb. The primary sources of uncertainty are of a statistical nature (3.3%), and the MC simulation of $t\bar{t}\gamma$ production with parton showering, which contributes 3.7%. The uncertainties associated with jet's properties are determined to be 3.0%, while the b-tagging uncertainty is 2.1%.

The differential cross sections as a function of the photon p_{T} are analysed within the SMEFT framework to set constraints on parameters pertinent to the electroweak dipole moments of the top quark. Although these constraints improve somewhat when the $t\bar{t}Z$ channel is included [11], this highlights the need for further combined measurements to achieve more significant results.

The precise test of the lepton flavour universality (LFU) for the centre-of-mass energy of 13 TeV using W-leptonic bosons produced from the decay of top pairs and an external measurement of $R_Z^{\mu\mu/ee}$ are studied in Ref. [12]. The ratio of the branching ratios of the W boson to muons and electrons, $R_W^{\mu/e} = \mathcal{B}(W \to \mu\nu)/\mathcal{B}(W \to e\nu)$ is determined. Background contributions are categorized into several sources, including Wt, $Z+$jets, dibosons, and events with misidentified leptons. Events include precisely two leptons (electrons or muons) with opposite charges.

The criteria for selecting leptons includes $p_{\mathrm{T}} > 27.3$ GeV and $|\eta| < 2.5$, while the b-tagged jets are required to have $p_{\mathrm{T}} > 30$ GeV and $|\eta| < 2.5$. An extra criterion is applied for the selection of lepton pairs: $m_{ll} > 30$ GeV is necessary for the $t\bar{t} \to llb\bar{b}\nu\bar{\nu}$ process, and for lepton pairs of the same flavour $(ee, \mu\mu)$, the condition 66 GeV $< m_{ll} <$ 116 GeV has to be satisfied for the inclusive $Z \to ll$ selection.

The $t\bar{t}$ production cross section is measured in different dilepton channels (ee, $e\mu$, and $\mu\mu$) by fitting the number of selected events with one or two b-tagged jets to theoretical predictions based on the assumed $t\bar{t}$ cross section and background estimates. The ratio $R_W^{\mu/e}$ is reported to be $R_W^{\mu/e} = 0.9995 \pm 0.0022(\text{stat.}) \pm 0.0036(\text{syst.}) \pm 0.0014(\text{ext.})$. Figure 3 shows the comparison of this measurement along with other previous results.

The systematic uncertainties due to the lepton identification and trigger efficiencies are minimized by normalizing the result to a simultaneous measurement of $R_Z^{\mu\mu/ee} = \mathcal{B}(Z \to \mu\mu)/\mathcal{B}(Z \to ee)$. The overall uncertain-

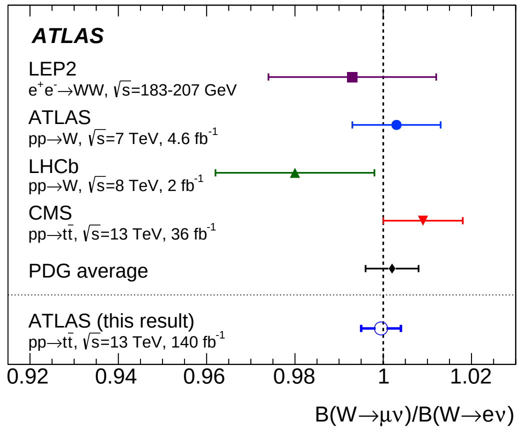

Fig. 3. Measurement of $R_W^{\mu/e}$ compared to previous results from LEP2, LHC experiments [12], and the PDG average [13].

ties associated with determining $\sigma_{t\bar{t}}$ and $\sigma_{Z\to ll}$ are determined to be 2.66% and 1.32%, respectively. This outcome aligns with the LFU assumption and represents the most accurate measurement available, featuring the reduced uncertainty compared to the previously established global average.

3. Quantum entanglement with top pairs at high energy

The quantum effects are also probed by the ATLAS Collaboration. The highest energy observation of the quantum entanglement in leptonic $t\bar{t}$ events produced at the LHC, with a centre-of-mass energy of 13 TeV, is reported [14].

The observable $D = -3\langle\cos\phi\rangle$ used to infer the quantum entanglement is defined in terms of the average value of the cosine of the angle between the charged lepton directions. The observable is measured in a narrow interval around the $t\bar{t}$ production threshold $340 < m_{t\bar{t}} < 380$ GeV (Region I), at which the entanglement detection is expected to be significant. Other regions, where no hint of entanglement is expected, are used as control ones: $380 < m_{t\bar{t}} < 500$ GeV (Region II) and $m_{t\bar{t}} > 500$ GeV (Region III). For Region I, the observed (expected) results are: $D = -0.537 \pm 0.002(\text{stat.}) \pm 0.019(\text{syst.})(-0.470 \pm 0.002(\text{stat.}) \pm 0.017(\text{syst.}))$.

These results are reported in a fiducial phase space, defined by the presence of exactly one electron and one muon with opposite electric charges, along with at least two particle-level jets, one of which must be b-tagged (*i.e.*, contain a b-hadron). The selection is based on stable particles to minimize uncertainties arising from the limitations of MC event generators and parton shower models in the simulation of top-quark pair production. This result deviates from the non-entanglement scenario by more than 5σ, establishing the formation of entangled $t\bar{t}$ states, constituting the first observation of entanglement in a quark–antiquark pair. The measurement in the top-quark sector not only enhances the understanding of quantum mechanics but also has far-reaching implications for high-energy physics and future research directions.

4. Top-pair production as a probe in heavy-ion collisions at the LHC

This contribution highlights two analyses: the first is based on a $p+\mathrm{Pb}$ collision dataset with an integrated luminosity of 165 nb^{-1} at $\sqrt{s_{NN}} = 8.16$ TeV (2016) [15], while the second is based on a Pb+Pb collision data sample with an integrated luminosity of 1.9 nb^{-1} at $\sqrt{s_{NN}} = 5.02$ TeV, collected in 2015 and 2018 [16]. In Ref. [15], the study focuses on measuring the nuclear modification factor for $t\bar{t}$ production in $p+\mathrm{Pb}$ collisions. The event selection follows two channels: the single-leptonic channel requires exactly one lepton (e or μ) with $p_{\mathrm{T}} > 15$ GeV and at least four jets (with at least one identified as a b-tag), while the dileptonic channel requires exactly two opposite-charge leptons with additional invariant mass cuts and at least two jets.

The top-quark pair production cross section is determined as $\sigma_{t\bar{t}} = \mu_{t\bar{t}}\, A_{\mathrm{Pb}}\, \sigma^{\mathrm{th}}_{t\bar{t}}$, where A_{Pb} is the mass number of lead and $\sigma^{\mathrm{th}}_{t\bar{t}}$ denotes the theoretical cross section. The normalization factor, $\mu_{t\bar{t}}$, defined as $\sigma_{t\bar{t}}/A_{\mathrm{Pb}}\, \sigma^{\mathrm{th}}_{t\bar{t}}$, for all channels is shown in figure 4 and is found to agree with the SM expectations. The result can be translated into an observed cross section of

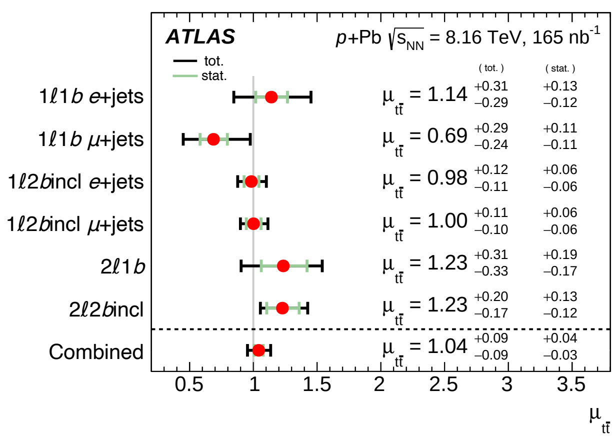

Fig. 4. The observed best-fit values of the signal strength $\mu_{t\bar{t}}$ and their uncertainties by final-state category and combined. The individual $\mu_{t\bar{t}}$ values for the channels are obtained from a simultaneous fit with the signal-strength parameter for each channel floating independently [15].

$\sigma_{t\bar{t}} = 58.1 \pm 2(\text{stat.})^{+4.8}_{-4.4}(\text{syst.})$ nb with a significance greater than 5σ in both channels, with a total uncertainty of 9%. The nuclear modification factor $R_{pA} = \sigma^{p+\text{Pb}}_{t\bar{t}}/A_{\text{Pb}}\,\sigma^{pp}_{t\bar{t}}$ is found to be $1.090 \pm 0.039(\text{stat.})^{+0.094}_{-0.087}(\text{syst.})$ nb, which is consistent with unity within the uncertainty. This measurement paves a new way to constrain nuclear PDFs in the region of high Bjorken-x and serves as an input for upcoming measurements involving the extraction of QGP properties in Pb+Pb collisions.

In Ref. [16], the presence of all quark flavours in the pre-equilibrium stage of the quark–gluon plasma (QGP)[2] is investigated. The event selection requires exactly one electron and one muon with an invariant mass $m(e\mu) >$ 30 GeV, along with at least two jets with $p_{\text{T}} \geq 35$ GeV. Centrality intervals are determined using the Glauber model, focusing on the 0–80% range to prevent the interference of photon-induced processes.

The theoretical cross section in pp collisions, scaled by the lead mass number, is $\sigma^{\text{th}}_{t\bar{t}} = 2.95^{+0.08}_{-0.10} \pm (\text{scale})^{+0.10}_{-0.09}(m_t)^{+0.21}_{-0.21}(\text{PDF} + \alpha_{\text{s}})$ μb and the measured inclusive cross section is $\sigma_{t\bar{t}} = 3.6^{+1.0}_{-0.9}(\text{stat.})^{+0.8}_{-0.5}(\text{syst.})$ μb. The overall relative uncertainty amounts to 31%, primarily attributed to the size of the dataset, with the statistical uncertainty being 26% and the systematic uncertainty 18%. These results agree well with SM predictions, indicating the presence of all quark flavours in the pre-equilibrium stage of QGP.

5. Conclusions

The results presented here pave the way for further investigations of the top-quark properties and their interactions within the ATLAS experiment. The full set of results can be found at the ATLAS top-quark group page[3]. With increased luminosity and improved detector capabilities of Run 3 and the High-Luminosity LHC, future measurements will achieve unprecedented precision, enabling a deeper exploration of the top-quark sector. These advancements could refine the understanding of fundamental forces and particles, test the limits of the SM, and potentially reveal new phenomena in high-energy physics.

This work was supported in part by the Ministry of Science and Higher Education, Poland, grant 2022/WK/08.

[2] Quark–Gluon Plasma is a state of matter in which quarks and gluons, normally confined within hadrons, are deconfined and free to move within a hot, dense medium.

[3] https://twiki.cern.ch/twiki/bin/view/AtlasPublic/TopPublicResults

REFERENCES

[1] J. Collins, «Foundations of Perturbative QCD», Cambridge Monographs on Particle Physics, Nuclear Physics and Cosmology, Vol. 32, *Cambridge University Press*, 2011.

[2] P.W. Higgs, *Phys. Lett.* **12**, 132 (1964).

[3] Particle Data Group (S. Navas *et al.*), *Phys. Rev. D* **110**, 030001 (2024).

[4] ATLAS Collaboration (G. Aad *et al.*), *J. Instrum.* **3**, S08003 (2008).

[5] ATLAS Collaboration (L. Evans, P. Bryant), *J. Instrum.* **3**, S08001 (2008).

[6] ATLAS Collaboration (G. Aad *et al.*), *Phys. Rev. D* **110**, 072010 (2024).

[7] ATLAS Collaboration (G. Aad *et al.*), *J. High Energy Phys.* **2025**, 068 (2025).

[8] ATLAS Collaboration, *Phys. Lett. B* **860**, 139177 (2025).

[9] ATLAS Collaboration (G. Aad *et al.*), *J. High Energy Phys.* **2024**, 182 (2024).

[10] ATLAS Collaboration (G. Aad *et al.*), *J. High Energy Phys.* **2024**, 191 (2024).

[11] ATLAS Collaboration (G. Aad *et al.*), *J. High Energy Phys.* **2024**, 163 (2024).

[12] ATLAS Collaboration (G. Aad *et al.*), *Eur. Phys. J. C* **84**, 993 (2024).

[13] Particle Data Group (R.L. Workman *et al.*), *Prog. Theor. Exp. Phys.* **2022**, 083C01 (2022).

[14] ATLAS Collaboration, *Nature* **633**, 542 (2024).

[15] ATLAS Collaboration (G. Aad *et al.*), *J. High Energy Phys.* **2024**, 101 (2024).

[16] ATLAS Collaboration (G. Aad *et al.*), *Phys. Rev. Lett.* **134**, 142301 (2025).